Supplementary Information

Modification of Cu-ZnO-ZrO$_2$ catalysts by La$_2$O$_3$ to quantitatively tune Cu$^+$-Cu^0 dual sites for hydrogenation of dimethyl adipate to produce 1,6-hexanediol

Xianlong Gao, Guoqing Zhao, Lei Miao, Lei Li and Zhirong Zhu*

(School of Chemical Science and Engineering, Tongji University, Shanghai 200092, P. R. China.)

*Corresponding author.
E-mail address: zhuzhirong@tongji.edu.cn (Z. Zhu).
Tel./fax: +8621-65982563.

Characterization of catalyst

X-ray diffraction (XRD) analysis was carried out on a X-ray diffraction (Rigaku D/Max-2500, Japan) using nickel filtered Cu Ka (λ= 0.15406 nm) radiation. The scan rate, diffraction range, tube voltage and tube current were 8 º/min, from 10 º to 80 º, 40 kV and 100 mA, respectively.

Nitrogen adsorption-desorption proles at -196 ºC were obtained by a Quantachrome Automated Gas Sorption apparatus (Micromeritics ASAP 2020). The samples were dehydrated at 300 ºC using vacuum degassing for 12 h before experiments. The specific surface area was calculated by the BET (Brunauer-Emmett-Teller) method.

Transmission electron microscopy (TEM) micrograph was obtained using a JEOL JEMF200 election microscope operating at 200 kV.

The elemental compositions of catalysts were measured by inductively coupled plasma optical emission spectroscopy (ICP-OES).

X-ray photoelectron spectroscopy (XPS) measurements were performed on Escalab 250 (Thermo Fisher VG) with a monochromatic X-ray source of Al Ka under ultra-high vacuum (2.4×10^{-8} Pa). The deconvolution method of XPS spectra was fitted by Gaussian function.

Thermo gravimetric analysis (TGA) of the spent catalyst was carried out on a METTLER TGA/DSC1/1600HT apparatus in air atmosphere at a heating rate of 10 ºC/min.

CO_2 temperature-programmed desorption (CO_2-TPD) was performed on a ChemBET Pulsar & TPR/TPD apparatus (Quantachrome Instruments) equipped with a TCD.

H_2 temperature-programmed desorption (H_2-TPD) was performed on a ChemBET Pulsar & TPR/TPD apparatus (Quantachrome Instruments) equipped with a TCD. 70 mg of the catalyst precursors was reduced in H_2-Ar gas (10% H_2, 30 ml·min^{-1}) at 350 ºC for 4 h firstly, and then cooled to 40 ºC under a He flow (30 ml·min^{-1}). Then, the sample adsorbed H_2 in a 10% H_2-He flow (30 ml·min^{-1}) for 60 min. Subsequently, the sample was purged by He flow (30 ml·min^{-1}) at 50 ºC for 60 min. After that, the H_2-TPD signal was recorded in a He flow by a TCD detector from 50 to 400 ºC at a heating rate of 10 ºC·min^{-1}.

The metallic copper surface areas and metal dispersions for samples were determined according to H_2-N_2O titration. The Cu-ZnO-ZrO_2-La_2O_3 catalysts were also characterized by N_2O chemisorption and H_2-TPR method using a Quantachrome chemisorption apparatus (ChemBET 3000, USA) with a TCD. Firstly, 50 mg of sample was pretreated in a N_2 flow at 350 ºC for 1 h, followed by reduction in a H_2-N_2 mixed flow (10% H_2, 30 ml·min^{-1}) at 350 ºC for 2 h and then cooled to 90 ºC under a N_2 flow (30 ml·min^{-1}). Next, 10% N_2O-90% He (30 ml·min^{-1}) was introduced at 90 ºC for 1h to oxidize Cu to Cu_2O. Then, H_2-TPR was conducted in H_2-N_2 mixed gas (10% H_2, 30 ml·min^{-1}) from 30 ºC to 400 ºC, and kept at 350 ºC for 1 h. Cu^0 surface area (S_{Cu}) was calculated according to $649 \times D_{Cu} \times$ Cu loading (wt%).

The reaction equation is as follows:

$$CuO + H_2 \rightarrow Cu + H_2O \tag{1}$$

$$2Cu + N_2O \rightarrow Cu_2O + N_2 \tag{2}$$

$$Cu_2O + H_2 \rightarrow 2Cu + H_2O \tag{3}$$

the amount of consumed H_2 in equation (1) was denoted as X, and the consumption of H_2 in equation (3) was denoted as Y.

Cu dispersion is:

D=(2Y/X) (4)

Correspondingly, metallic Cu surface area (S_{Cu}, m^2/g) was calculated as the following equation:

$$S_{Cu} = \frac{D_{Cu} * N_{av}}{S_{Cu} * \rho_{Cu}} \approx 649 \times D_{Cu} \tag{5}$$
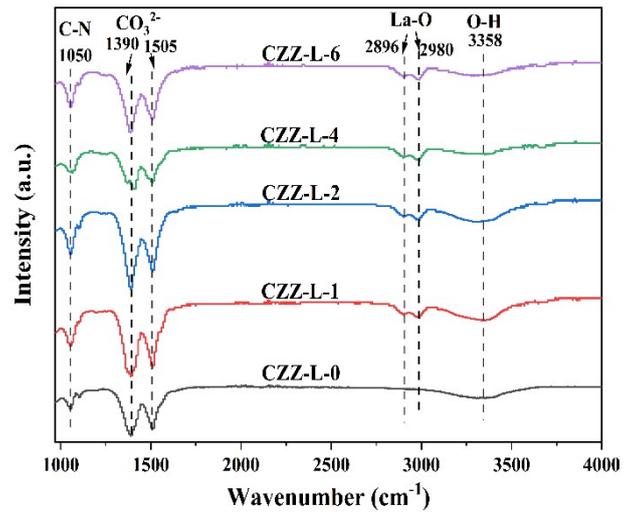
Fig. S1 FT-IR results of the precursors of the different Cu-ZnO-ZrO$_2$-La$_2$O$_3$ catalysts.
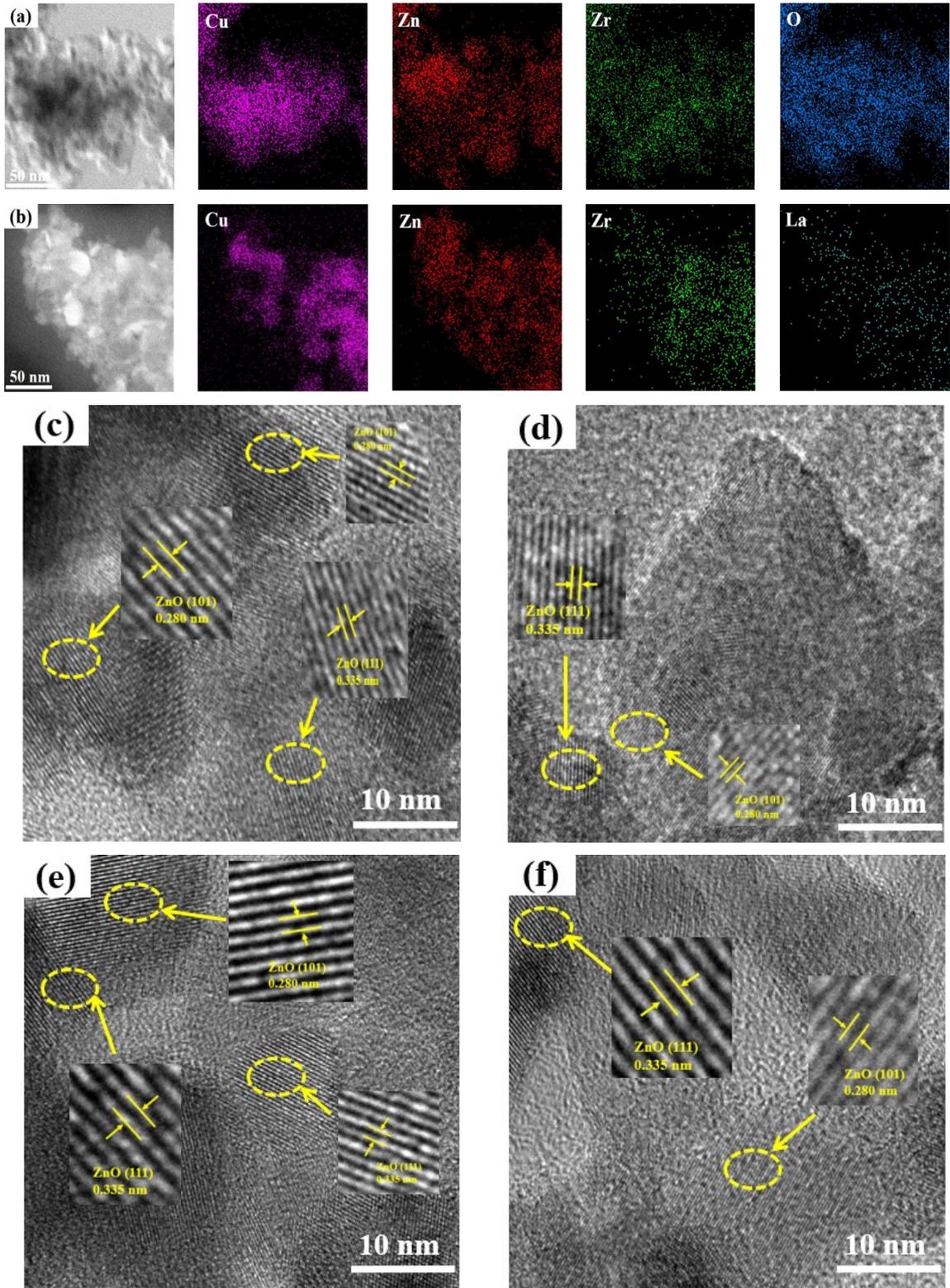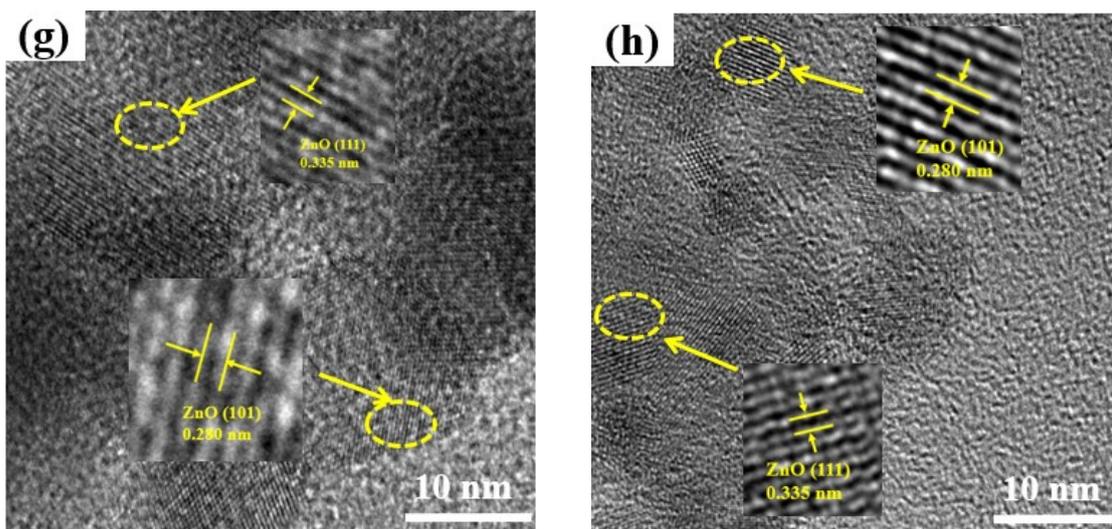
Fig. S2 (a) HAADF-STEM image of the CZZ-L0-CP catalyst and the corresponding elemental maps of Cu, Zn, Zr and O. (b) HAADF-STEM image of the CZZ-L2-CP catalyst and the corresponding elemental maps of Cu, Zn, Zr and La. (c) HRTEM image of CZZ-L0-CP. (d) HRTEM image of CZZ-L1-CP. (e) HRTEM image of CZZ-L2-CP. (f) HRTEM image of CZZ-L4-CP. (g) HRTEM image of CZZ-L6-CP. (h) HRTEM image of CZZ-L2-IM.
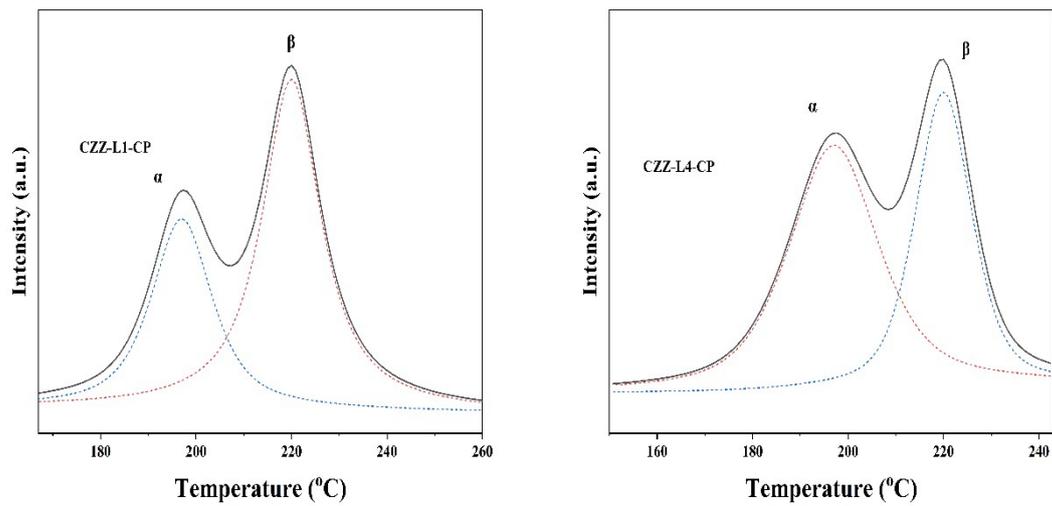
Fig. S3 Results of H$_2$-TPR fitting for CZZ-L1-CP and CZZ-L4-CP catalysts.
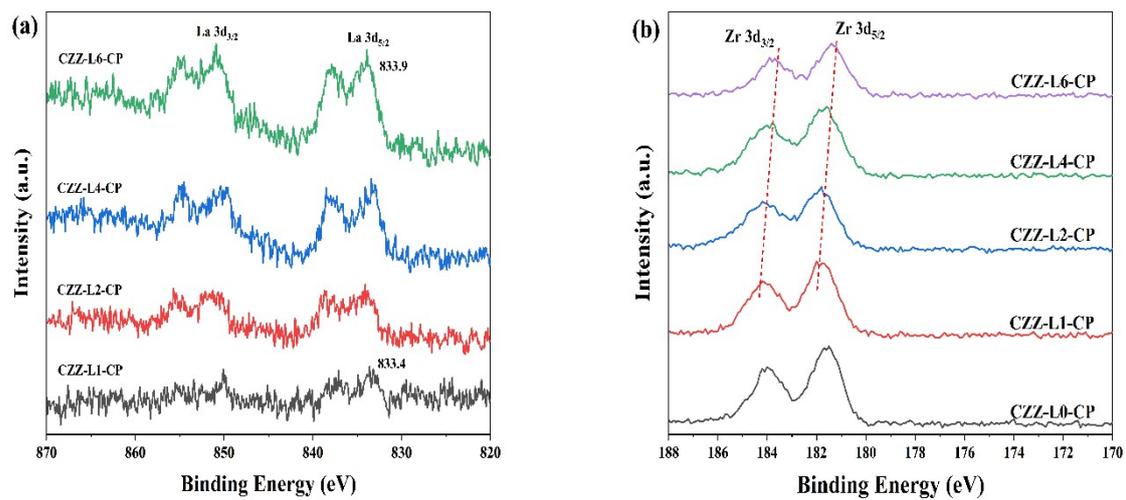
Fig. S4 (a) La 3d XPS spectra. (b) Zr 3d XPS spectra spectra.
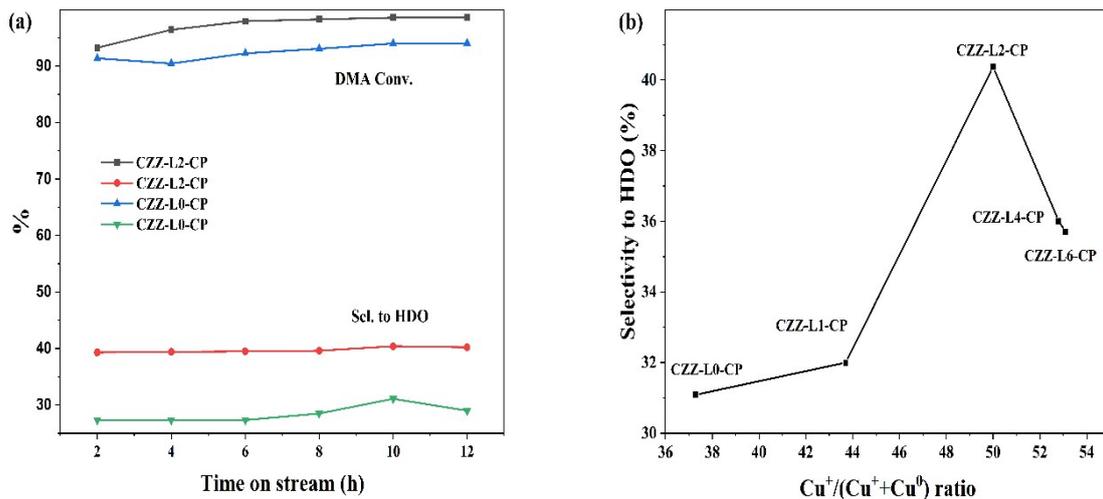
Fig. S5 (a) The conversion of DMA and selectivity of HDO of the CZZ-L0-CP and CZZ-L2-CP catalysts for DMA hydrogenation reaction as a function of the time on stream. (b) The correlation of HDO selectivity with $Cu^+/(Cu^++Cu^0)$. Reaction conditions: 8 g of catalyst, 250 ºC, 4 MPa H_2, H_2/DMA = 10 (mol·mol^{-1}), WHSV$_{DMA}$ = 0.5 g·g$_{cat}^{-1}$·h^{-1}.
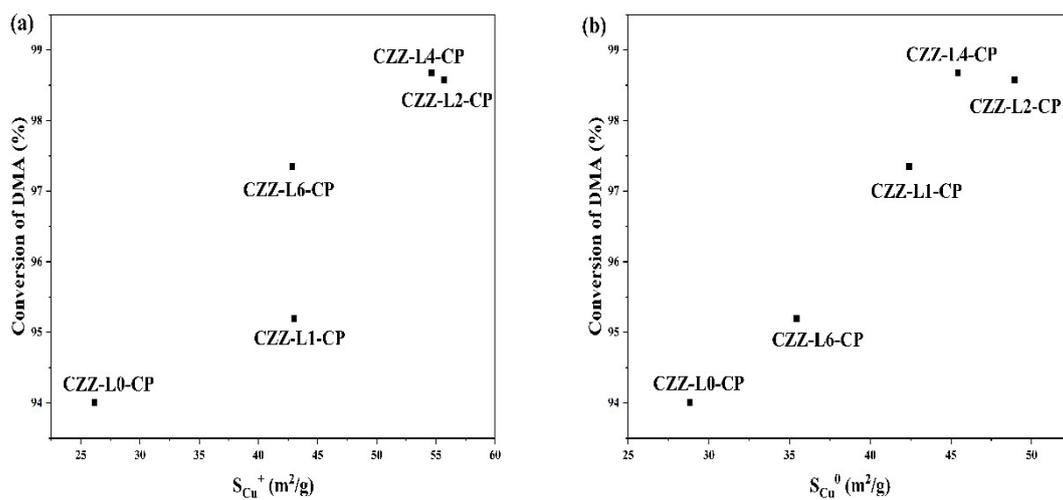
Fig. S6 The correlation of DMA conversion with over Cu^+ (a) and Cu^0 (b) sites plotted along the surface area of Cu^+ and Cu^0 species
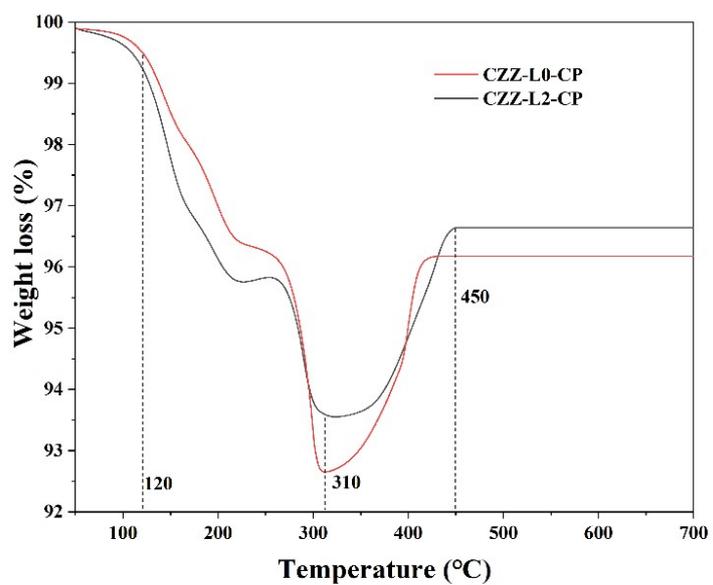
Fig S7 TG profiles of the CZZ-L0-CP and CZZ-L2-CP catalysts after reaction at 250 °C for 12 h.

Table S1 The structural properties of as-calcined samples

Samples	S_{BET}[a] $(m^2 \cdot g^{-1})$	$V_{p, BJH}$[b] $(cm^3 \cdot g^{-1})$	$d_{p, BJH}$[c] (nm)	Cu loading (wt%)[d]	Zn loading (wt%)[d]	La loading (wt%)[d]	Crystallite Size of CuO (nm) by XRD[e]
CZZ-L0-CP	20.6	0.096	18.58	41.9	22.9	0	17
CZZ-L1-CP	32.5	0.147	18.13	41.7	22.2	0.98	14
CZZ-L2-CP	41.1	0.212	20.69	41.3	21.8	1.99	14
CZZ-L4-CP	31.7	0.203	25.59	40.5	20.8	4.01	14
CZZ-L6-CP	23.3	0.143	24.47	39.0	20.3	5.99	15
CZZ-L2-IM	14.6	0.081	22.13	41.2	21.9	2.31	15

[a] S_{BET}=Specific Surface Area.
[b] $V_{p, BJH}$=Total Pove Volume Measured at P/P_0=0.99.
[c] $d_{p, BJH}$=Average BJH adsorption Pore Diameter.
[d] Determined by ICP-OES.
[e] CuO crystallite size was calculated by the Scherrer equation at 2θ=38.8 °.

Table S2 Physicochemical properties of various CZ-M catalysts

Samples	Cu loading (wt%) [a]	Crystallite Size (nm)	
		by XRD [b]	by N_2O
CZZ-L0-CP	47.5	28	10.8
CZZ-L1-CP	46.0	24	7.04
CZZ-L2-CP	45.4	19	6.02
CZZ-L4-CP	44.5	19	6.37
CZZ-L6-CP	43.7	26	8.00
CZZ-L2-IM	45.2	34	16.1

[a] Determined by ICP-OES

[b] Cu crystallite size was calculated by the Scherrer equation at $2\theta=43.2$ °

Table S3 Characterization of Cu species for the CZ-X catalysts

Samples	S_{BET} $(m^2 \cdot g^{-1})$ [a]	$V_{p, BJH}$ $(cm^3 \cdot g^{-1})$ [b]	$d_{p, BJH}$ (nm) [c]	D_{Cu}[d] (%)	D_{Cu}[f] (%)
CZZ-L0-CP	11.6	0.054	18.60	9.3	3.57
CZZ-L1-CP	23.1	0.084	14.51	14.2	3.57
CZZ-L2-CP	28.8	0.166	23.11	16.6	5.26
CZZ-L4-CP	26.0	0.100	15.70	15.7	5.26
CZZ-L6-CP	15.4	0.046	11.94	12.5	3.33
CZZ-L2-IM	6.5	0.033	20.67	6.9	2.94

[a] S_{BET}=Specific Surface Area.

[b] $V_{p, BJH}$=Total Pove Volume Measured at P/P_0=0.99.

[c] $d_{p, BJH}$=Average BJH adsorption Pore Diameter.

[d] Cu dispersion obtained by N_2O titration.

[e] Cu dispersion obtained by D_{Cu} (%)=1.0/d_{Cu} (nm) (d_{Cu}: mean Cu particle size from XRD results).

Table S4 center of reduction peaks and their contributions to the TPR pattern over CZZ-LX catalysts with different La loading

Samples	TPR peak position [temperature (°C)] and concentration (%) [a]		
	Peak α	Peak β	Peak γ
CZZ-L0-CP	-	215 (100)	-
CZZ-L1-CP	197 (64.2)	220 (35.8)	-
CZZ-L2-CP	190 (100)	-	-
CZZ-L4-CP	197 (58.1)	220 (41.9)	-
CZZ-L6-CP	-	-	285 (100)
CZZ-L2-IM	-	-	289 (100)

[a] Values in parentheses are the contributions (%) of each species.

Table S5 H$_2$-TPR results for Cu-ZnO-ZrO$_2$-La$_2$O$_3$ samples

Samples	Cu content [a] (wt%)	Amount of H$_2$ consumption [b] (mmol·g$_{cat}^{-1}$)	Stoichiometry of H$_2$ [c] (mmol·g$_{cat}^{-1}$)
CZZ-L0-CP	47.5	1.96	7.48
CZZ-L1-CP	46.0	1.81	7.24
CZZ-L2-CP	45.4	1.68	7.15
CZZ-L4-CP	44.5	1.45	7.01
CZZ-L6-CP	43.7	1.39	6.88
CZZ-L2-IM	45.2	1.72	7.12

[a] Determined by ICP-OES.

[b] Amount of H$_2$ consumption was determined from H$_2$-TPR results.

[c] Stoichiometry of H$_2$ consumption was calculated for reduction of Cu species to Cu^0 based on the actual Cu content (the atomic ratio between H$_2$ and Cu species is 1:1).

Table S6 Characterization of Cu species and surface atom concentrations for the CZZ-LX catalysts

Samples	$S_{Cu^0}{}^a$ $(m^2 \cdot g^{-1})$	$S_{Cu^+}{}^b$ $(m^2 \cdot g^{-1})$	$X_{Cu^+}{}^b (\%)$	$X_{Ov}{}^d (\%)$	$X_{Zr^{3+}}{}^e (\%)$	$STY_{HDO}{}^f$ $(g \cdot g_{cat}{}^{-1} \cdot h^{-1})$
CZZ-L0-CP	28.81	26.14	37.3	53.5	-	9.91
CZZ-L1-CP	42.41	42.85	43.7	45.4	19.0	10.56
CZZ-L2-CP	48.94	55.69	50.0	61.8	22.6	13.51
CZZ-L4-CP	45.34	54.64	52.8	50.2	16.1	12.85
CZZ-L6-CP	35.45	43.00	53.1	45.9	13.8	12.07

[a] Metallic copper surface area determined by H_2-N_2O titration.

[b] $S_{Cu^+} = Cu^+$ Surface area, calculated on the basis of X_{Cu^+} and S_{Cu^0}.

[c] X_{Cu^+} represents $Cu^+/(Cu^+ + Cu^0)$ ratio calculated from Cu LMM spectra.

[d] X_{Ov} represents $O_{vac}/(O_{latt} + O_{vac} + O_{ads})$ ratio calculated from XPS.

[e] $X_{Zr^{3+}}$ represents $Zr^{3+}/(Zr^{3+} + Zr^{4+})$ ratio calculated from XPS.

[f] STY_{HDO} is denoted as the space time yield of HDO and calculated as gram of HDO per gram of catalyst per hour $(g \cdot g_{cat}{}^{-1} \cdot h^{-1})$.

Table S7 The temperatures and areas of CO_2 desorption peaks with different La loadings

Samples	T/°C	A/(a.u.)	Ratio/%
CZZ-L0-CP	81	77.7	100
CZZ-L1-CP	86	83.4	107
CZZ-L2-CP	97	130.3	168
CZZ-L4-CP	86	114.2	147
CZZ-L6-CP	80	67.8	87
CZZ-L2-IM	75	56.1	72